

Analyzing Well Production Data Using Combined-Type-Curve and Decline-Curve Analysis Concepts

Ram G. Agarwal, SPE, David C. Gardner, SPE, Stanley W. Kleinsteiber, SPE, and Del D. Fussell,* SPE,
Amoco Exploration & Production Co.

Summary

This paper presents new production decline curves for analyzing well production data from radial and vertically fractured oil and gas wells. These curves have been developed by combining decline-curve and type-curve analysis concepts to result in a practical tool which we feel can more easily estimate the gas (or oil) in place as well as to estimate reservoir permeability, skin effect, fracture length, conductivity, etc. Accuracy of this new method has been verified with numerical simulations and the methods have been used to perform analyses using production data from several different kinds of gas wells. Field and simulated examples are included to demonstrate the applicability and versatility of this technology.

These new production decline-type curves represent an advancement over previous work because a clearer distinction can be made between transient- and boundary-dominated flow periods. They also provide a more direct and less ambiguous means of determining reserves. The new curves also contain derivative functions, similar to those used in the pressure transient literature to aid in the matching process. These production decline curves are, to our knowledge, the first to be published in this format specifically for hydraulically fractured wells of both infinite and finite conductivity. Finally, these new curves have been extended to utilize cumulative production data in addition to commonly used rate decline data.

Introduction

Estimation of hydrocarbon-in-place and reserves for oil and gas reservoirs is needed from the time when such reservoirs are first discovered to future times when they are being developed by drilling step-out wells or infill wells. These estimates are needed to determine the economic viability of the project development as well as to book reserves required by regulatory agencies.

During the last 50 years, various methods have been developed and published in the literature for estimating reserves from high-permeability oil reservoirs to low-permeability gas reservoirs. These methods range from the basic material balance methods to decline-type curve analysis techniques. They have varying limitations and are based on analytical solutions, graphical solutions (known as type curves and decline curves), and combinations of the two. Examples of these range from Arp's¹ decline equations for liquids to Fetkovich's² liquid decline curves, Carter's³ gas type curves, and Palacio and Blasingame** gas equivalent to liquid decline curves. Other papers on this subject, too many to quote here, have appeared in the SPE literature.

Type-curve analysis methods have become popular, during the last 30 years, to analyze pressure transient test (e.g., buildup, drawdown) data. However, pressure transient data can be costly to

obtain and may not be available for many wells, while well production data are routinely collected and are even available from industry databases. In the absence of pressure transient data, a method that can use readily available well production data to perform pressure transient analysis would be very beneficial. The result is the development of these new production decline-type curves.

Purpose

The purpose of this paper is to document new production decline-type curves for estimating reserves and determining other reservoir parameters for oil and gas wells using performance data. Depending on the amount of performance data available, these methods can provide lower-bound and/or upper-bound estimates of a well's hydrocarbon-in-place. The accuracy of such estimates for reserves and other reservoir parameters will depend on the quality and kind of the performance data available.

It will be demonstrated and confirmed, using the methods of Palacio and Blasingame,** that solutions for constant rate or constant bottomhole pressure production for oil and gas wells can be converted, in most cases, to equivalent constant rate liquid solutions.

First, we will review background material. Next, we will briefly discuss various methods which are commonly used for estimating gas reserves. Finally, we will present the new production decline-type curves and demonstrate their utility and application by means of both synthetic and field examples. Although the technology discussed in this paper is applicable to both oil and gas wells, our discussion will be limited mainly to gas wells.

Background Material

Transient and Pseudo-Steady-State Flow Conditions. When a well is first opened to flow, it is under a transient condition. It remains under this condition until the production from the well affects the total reservoir system. Then, the well is said to be flowing under a pseudo-steady-state (pss) condition or a boundary-dominated flow condition. Transient rate and pressure data are used to determine reservoir permeability and near-wellbore condition (damage or improvement), fracture length, and/or fracture conductivity, whereas pss data are required to estimate the fluid-in-place and reserves. Transient and pss flow conditions are schematically shown on a Cartesian graph in **Fig. 1** and on a log-log graph in **Fig. 2**.

Review of Various Reserve Estimation Methods. The volumetric method is used to make an initial estimate of gas-in-place using petrophysical data such as hydrocarbon porosity, pay thickness, initial reservoir pressure, reservoir temperature, pressure-volume-temperature (PVT) data, and reservoir size (or well spacing). Such estimates are useful and should be made whenever possible.

The material balance method for gas wells makes use of the material balance equation, $\bar{p}/\bar{z} = (p_i/z_i)(1 - (G_p/G_i))$ and the material balance graph, where \bar{p}/\bar{z} is plotted as a function of cumulative gas production. Although the material balance graph may have a limited application in certain cases (for example, tight

*Now retired.

Copyright © 1999 Society of Petroleum Engineers

This paper (SPE 57916) was revised for publication from paper SPE 49222, prepared for presentation at the 1998 SPE Annual Technical Conference and Exhibition, New Orleans, 27-30 September. Original manuscript received for review 30 November 1998. Revised manuscript received 7 July 1999. Paper peer approved 13 July 1999.

**Palacio, J.C. and Blasingame, T.A.: "Decline-Curve Analysis Using Type Curves: Analysis of Gas Well Production Data," paper SPE 25909 presented at the 1993 Rocky Mountain Regional Meeting/Low Permeability Reservoirs Symposium and Exhibition, Denver, Colorado, 26-28 April.

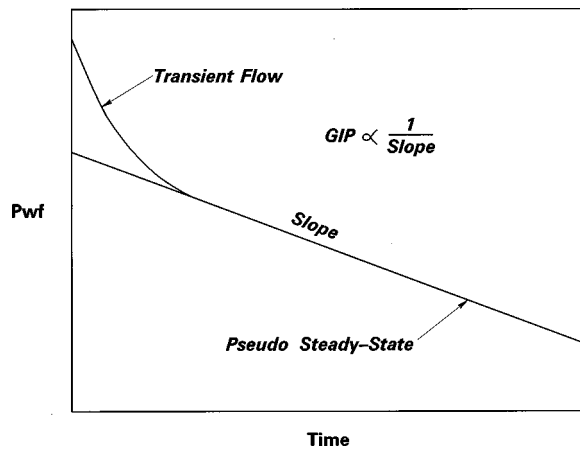


Fig. 1—Schematic plot of pressure drawdown data (Cartesian graph).

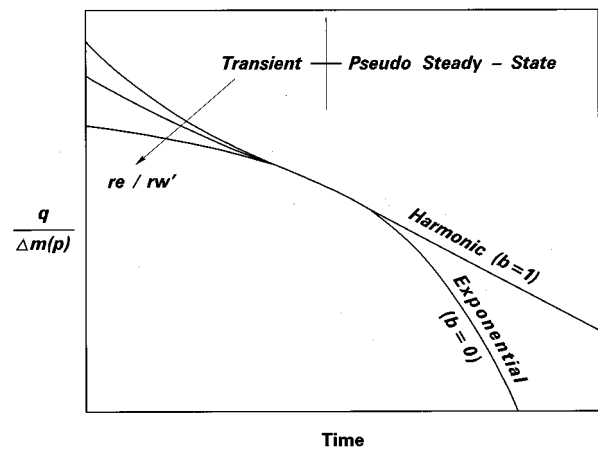


Fig. 2—Schematic plot of decline curves (log-log graph).

gas wells) it provides useful guidelines for reserves and can also give insight regarding the drive mechanism of a reservoir.

The reservoir limit test is based on the constant rate drawdown solution. A well is produced at a constant rate and the wellbore pressure response is plotted as a function of time on a Cartesian graph (see Fig. 1). During the pss condition, the slope of this line is inversely proportional to the fluid-in-place. This kind of test is not limited to, but is usually run on new exploration type wells for estimating reserves.

Arp's decline equation is based on empirical relationships of rate versus time for oil wells and is shown below:

$$q(t) = \frac{q_i}{(1 + bD_{it})^{1/b}} \quad (1)$$

In Eq. (1), $b=0$ and $b=1$ represent exponential and harmonic decline, respectively. During pss for liquid systems, an exponential decline is a characteristic of constant pressure production whereas a harmonic decline occurs with constant rate production. Any other value of b represents a hyperbolic decline (see Fig. 2). Although Arp's equation is strictly applicable for pss conditions, it has often been misused for oil and gas wells whose flow regimes are in a transient state.

Fetkovich liquid system decline curves were published in 1980 for analyzing oil wells producing at a constant pressure. He com-

bined the early time, transient, analytical solutions with Arp's equations for the later time, pseudo-steady-state solutions. A reproduction of his type curves is shown in Fig. 3.

Although the value of the b stem ranges from 0 to 1, curves for values of b greater than 1 are often added to Fig. 3 and are misused to match transient data. These liquid system curves are not recommended for gas wells especially when the magnitude of pressure drawdown is moderate to large. However, these curves ($b=0$ and $b=1$) may be used for gas wells if gas well data are converted to equivalent liquid system data. This concept has been used in this study and will be discussed later.

Carter gas system type curves, shown in Fig. 4, were developed in 1985 for gas wells producing at constant pressure to fill the gap which existed with the Fetkovich decline curves. Carter used a variable λ , reflecting the magnitude of pressure drawdown. The $\lambda=1.0$ curve assumes a negligible drawdown effect and corresponds to the $b=0$ on the Fetkovich liquid decline curves and represents a liquid system with an exponential decline. Curves with $\lambda=0.75$ and 0.55 are for gas wells with medium and large amounts of pressure drawdown. These type curves are better suited to estimate reserves for gas wells.

Palacio and Blasingame type curves, shown in Fig. 5, first presented in 1993, provide a major advancement in the area of analyzing oil and/or gas well performance data using type curves. Their paper is an excellent culmination of their work and the work

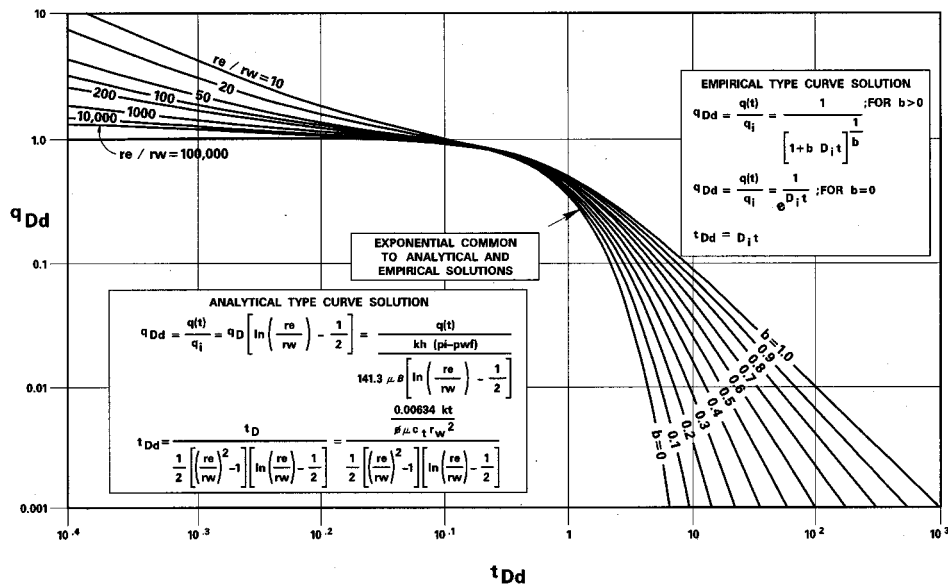


Fig. 3—Fetkovich liquid system decline curves (Ref. 2).

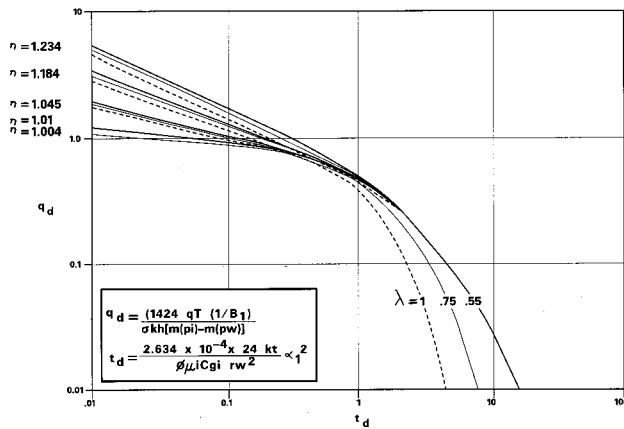


Fig. 4—Carter's constant pressure production type curves for gas systems (Ref. 3).

of other investigators whose goals were to convert gas well production data into equivalent constant rate liquid data. They also established a clear relationship among the previously discussed decline curves.

Palacio-Blasingame type curves provide a useful tool to estimate gas-in-place (GIP), reservoir permeability and skin. However, the transient stems are strictly valid only for radial flow and thus may not be suitable for analyzing gas wells with relatively long vertical hydraulic fractures of infinite or finite conductivity. It can also be difficult to pick up a clear transition between the transient and the pss flow periods from these and the other previously discussed decline curves. Palacio-Blasingame utilize derivative methods to facilitate the type-curve matching process. However, their approach results in multiple derivative curves, even for the radial flow system. Details about their type curves as well as a comprehensive list of pertinent references on this subject can be found in their paper.**

Discussion

Our first objective with this study was to verify, using a single-phase finite-difference reservoir simulator, a major finding of Palacio and Blasingame, that constant rate and constant bottom-hole pressure (BHP) solutions for liquid and gas systems, can be converted to an equivalent constant rate liquid solution. Constant rate liquid solutions are well understood for both transient and pss conditions and are widely used for pressure transient analysis (PTA) purposes. With constant rate liquid solutions, one can take advantage of the many well-known PTA techniques for plotting decline-curve data on different types of graph papers and for utilizing appropriate plotting variables such as pressure, rate, cumulative production, and time functions, and also the appropriate derivative functions.

Plotting Dimensionless Variables. Constant rate liquid solutions are commonly used for pressure transient analysis. Dimensionless variables, which are frequently used in type curves for pressure transient analysis, are dimensionless pressure p_{wD} and its derivatives with respect to dimensionless time dp_{wD}/dt_D , and with respect to log of dimensionless time $dp_{wD}/d \ln t_D$. To make a type curve graph appear like a decline curve, one can use the reciprocals of p_{wD} to produce graphs of $1/p_{wD}$ and $1\{dp_{wD}/d \ln t_D\}$ plotted against dimensionless time. The reciprocal log time derivative $1\{dp_{wD}/d \ln t_D\}$ does for the rate decline plot what $dp_{wD}/d \ln t_D$ does for the pressure buildup plot, namely, helping to identify flow regimes and to estimate permeability.

**Palacio, J.C. and Blasingame, T.A.: "Decline-Curve Analysis Using Type Curves: Analysis of Gas Well Production Data," paper SPE 25909 presented at the 1993 Rocky Mountain Regional Meeting/Low Permeability Reservoirs Symposium and Exhibition, Denver, Colorado, 26–28 April.

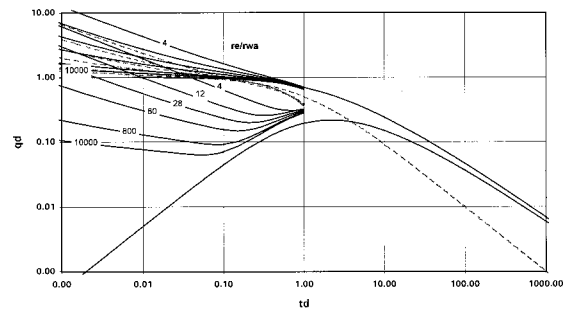


Fig. 5—Palacio-Blasingame radial system type curves**; radial transient stems 4, 12, 28, 80, 800, and 10,000.

References to these two types of derivatives are used quite extensively in this paper, so for convenience in the text and in the figures, a shorthand form representing the derivatives is used. PwD' is defined as the derivative of p_{wD} with respect to the independent variable. For example, with t_D as the independent variable, $PwD' = dp_{wD}/dt_D$ and $1/d \ln PwD' = 1\{dp_{wD}/d \ln t_D\}$.

Equivalence Between Constant Rate and Constant BHP Liquid Solutions. To demonstrate this, two radial liquid system cases were considered. The two systems were identical, except in one case (LR) the well was produced at a constant rate and in the other case (LP) the well was produced at a constant bottomhole pressure.

Fig. 6 shows graphs for both cases in terms of $1/p_{wD}$, PwD' , and $1/d \ln PwD'$. A comparison of these two cases shows that during the transient period, the two sets of results are very similar. However, they are quite different during the pseudo-steady-state (or boundary-dominated flow period). This is to be expected since constant rate solutions during the pss period show a harmonic decline (straight line with negative unit slope on log-log paper), whereas constant bottomhole pressure solutions result in an exponential decline (concave line on log-log paper). If constant BHP results are replotted using a modified time, $t_e = (\text{cumulative production})/(\text{instantaneous rate})$ and compared with the constant rate solutions, they become equivalent. This equivalence between the two solutions is shown in Fig. 7. Notice that during transient flow, PwD' has a negative unit slope, while $1/d \ln PwD'$ has a zero slope and a constant value of 2.0. During pss flow their roles reverse, that is, $1/d \ln PwD'$ has a negative unit slope, while PwD' has a constant value which is inversely proportional to GIP. Therefore, it is possible to estimate GIP and to determine whether this value is a lower- or upper-bound estimate.

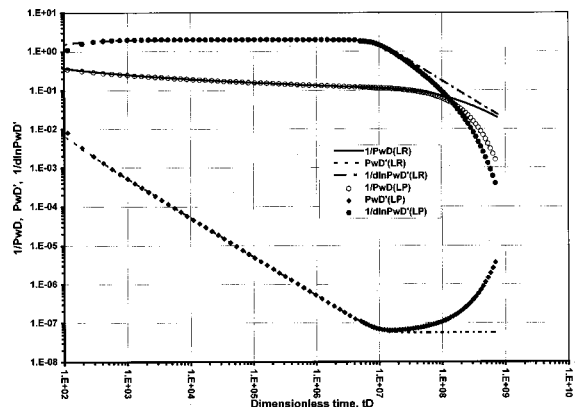


Fig. 6—Comparison of constant rate and constant BHP liquid production data, radial case.

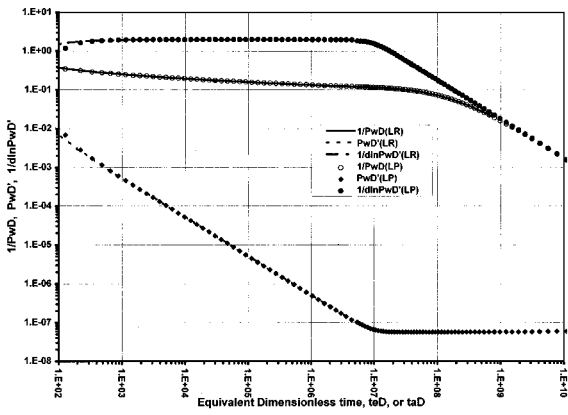


Fig. 7—Converting constant rate and constant BHP Data to an equivalent constant rate liquid data, radial case.

Equivalence Between Constant Rate and Constant BHP, Gas Solutions. To illustrate this equivalence, two radial gas system cases, constant rate case (GR) and constant BHP case (GP) were considered. Except for the mode of production, the two systems were identical. These cases should provide a difficult litmus test for verifying the desired equivalence. Fig. 8 shows graphs for both gas cases and is similar to Fig. 6 in terms of plotting variables. During the transient period, both constant rate and constant BHP cases appear identical. However, the difference between the two cases during the pss period becomes significant. This is to be expected because additional complications are caused not only by differences in modes of production but also by varying gas properties. We go through the conversion to an equivalent constant rate liquid solution in a stepwise manner. First, we use the dimensionless time based on the modified time t_e instead of real time as was done for the liquid cases. The second step is to redefine time in terms of pseudotime where the gas properties product (μc_g) is calculated as a function of average reservoir pressure \bar{p} . Pseudo-equivalent time t_a was developed by Palacio and Blasingame by extending earlier work of Fraim and Wattenbarger⁴ and is shown below:

$$t_a = \frac{1}{q(t)} (\mu c_g)_i \int_0^t \frac{q(t') dt'}{\mu(\bar{p}) c_g(\bar{p})} = \frac{1}{q(t)} (\mu c_g)_i \frac{Z_i G_i}{2P_i} \Delta[m(\bar{p})]. \quad (2)$$

Results after this conversion is made are found to be identical to those shown in Fig. 7. That is, the two gas cases become identical during both the transient and pss periods. This verifies that it is possible to convert constant BHP liquid as well as constant rate and constant BHP gas cases into an equivalent constant rate liquid

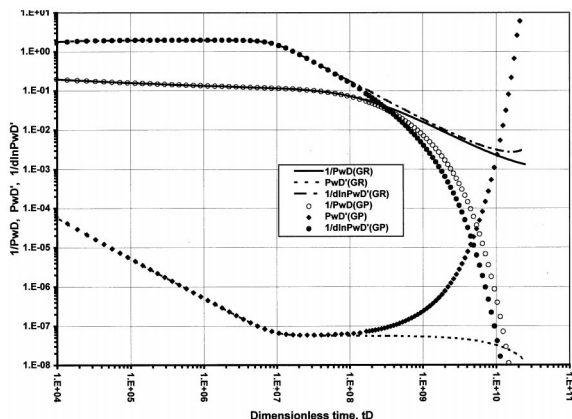


Fig. 8—Comparison of constant rate and constant BHP gas production data, radial case.

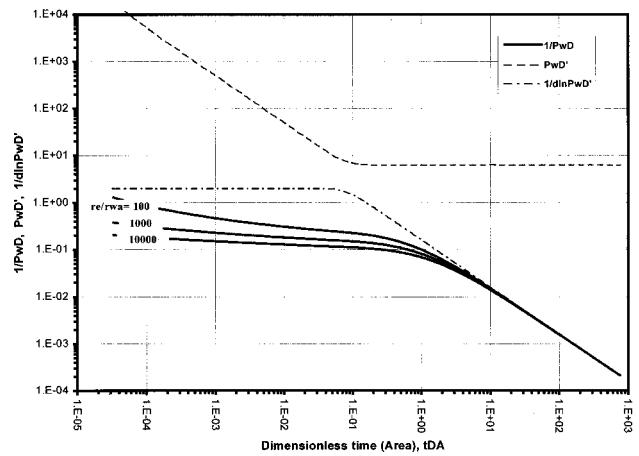


Fig. 9—Rate-time production decline-type curves for radial systems using t_D based on area ($r_e/r_{wa}=100, 1,000, 10,000$).

case. This is significant because it will permit us to focus our attention to mainly constant rate liquid systems. We have also found that for gas wells, where both the rate and pressure vary such that $1/p_{wD}$ is monotonically decreasing, the data can still be converted into the constant rate liquid analogue.

However, there is a computational problem. The calculation of pseudotime in Eq. (2) assumes that we know GIP (a parameter value we normally do not know and would like to determine). The implication of this assumption suggests an iterative procedure for determining GIP. This can be easily accomplished using a spreadsheet program and the method outlined in this paper.

Production Decline-Type Curves. These new decline-type curves will be presented under three categories: (1) *rate-time*, (2) *rate-cumulative production*, and (3) *cumulative production-time*. Under each category, we will present decline-type curves for radial systems and for vertically fractured wells with infinite and finite fracture conductivity, as appropriate.

Rate-Time Production Decline-Type Curves. Radial System. For the radial system log-log type curves, we generated three cases corresponding to $r_e/r_{wa} = 100, 1,000, \text{ and } 10,000$ and utilized the previously discussed approach for plotting the results. Dimensionless time variable for the x axis was calculated in two different ways: (1) based on the drainage area, A , and (2) the effective wellbore radius squared, r_{wa}^2 . Results are shown in Figs. 9 and 10, respectively.

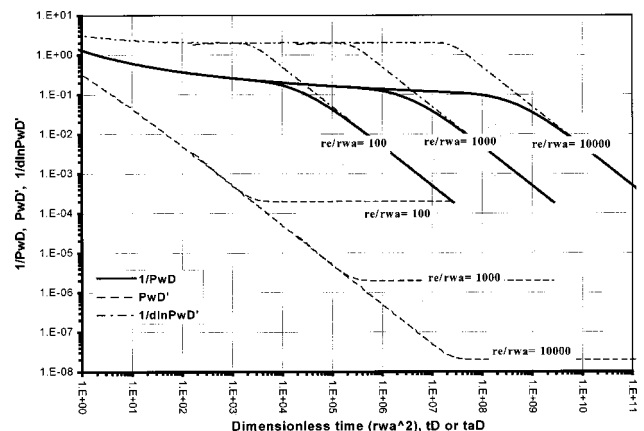


Fig. 10—Rate-time production decline-type curves for radial systems using t_D based on r_{wa} ($r_e/r_{wa}=100, 1,000, 10,000$).

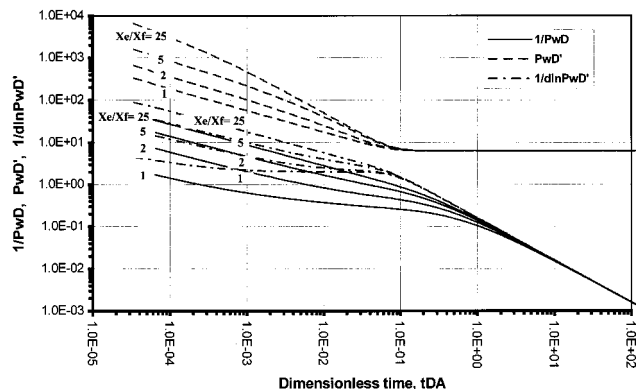


Fig. 11—Rate-time production decline-type curves for infinite conductivity fracture using t_D based on area ($x_e/x_f = 1, 2, 5, 25$).

In Fig. 9, where data have been plotted as a function of dimensionless time based on the area (A), $1/p_{wD}$ is a function of r_e/r_{wa} during the transient flow period. However, these different $1/p_{wD}$ curves merge together during the pss flow period and take on a unit slope. This graph looks similar to the decline curves published by Fetkovich, Carter, Palacio-Blasingame, and others, but has certain distinct advantages. A single curve is obtained for each of the two derivatives for all r_e/r_{wa} values. During the transient period, $1/d \ln PwD'$ has a constant value of 2.0 (zero slope), while PwD' has a negative unit slope. These characteristics are reversed during the pss period where $1/d \ln PwD'$ has the negative unit slope while PwD' has a constant value of 2π and a zero slope. This negative unit slope behavior is also referred to as harmonic decline. Both time and log time derivatives on log-log graphs are very useful because of their distinguishing features during transient and pss flow periods. This kind of graph is also useful for estimating gas-in-place.

In Fig. 10, where data have been plotted using dimensionless time based on r_{wa}^2 , a single curve is obtained during the transient flow period for $1/p_{wD}$ for all r_e/r_{wa} values and also there is a single curve for each of the two types of derivatives. However, these curves start peeling off for each r_e/r_{wa} value during the pss period. This kind of type curve graph is useful for estimating reservoir parameters such as permeability and skin effect.

Infinite Conductivity Fracture. Figs. 11 and 12 show similar graphs but for vertically fractured wells with infinite conductivity fractures. Here, data are plotted in a manner similar to Figs. 9 and 10. The main differences are that x_e/x_f (or \sqrt{A}/x_f) has been used as the parameter to replace r_e/r_{wa} (or \sqrt{A}/r_{wa}) that was used for

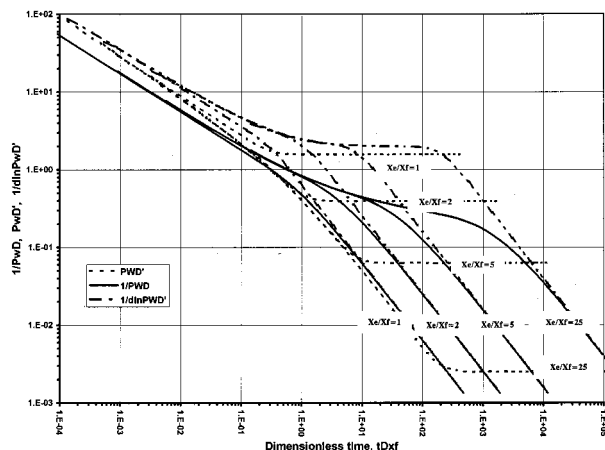


Fig. 12—Rate-time production decline-type curves for infinite conductivity fracture using t_D based on x_f ($x_e/x_f = 1, 2, 5, 25$).

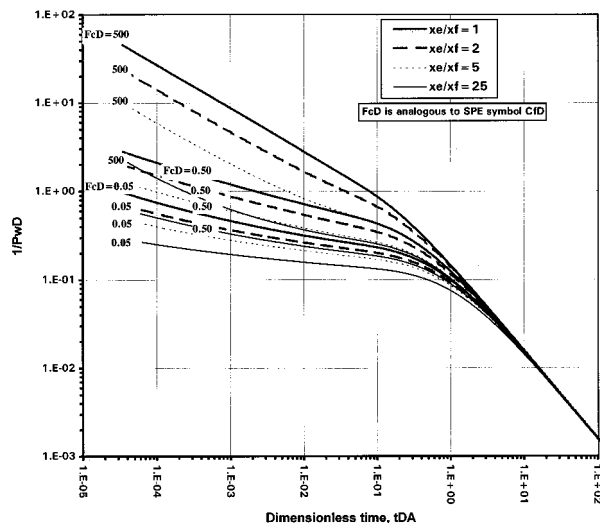


Fig. 13—Rate-time production decline-type curves for finite conductivity fracture using t_D based on area ($x_e/x_f = 1, 2, 5, 25$ and $F_{CD} = 0.05, 0.5, 500$).

the radial system cases. And the dimensionless time is based on the fracture half length x_f instead of r_{wa} . Values for x_e/x_f of 1, 2, 5, and 25 are shown. Comparison of Figs. 9 and 11 shows that multiple derivative curves are obtained for a fractured well as opposed to a single curve for the radial case.

Finite Conductivity Fracture. Figs. 13 and 14 show graphs of $1/p_{wD}$ and $1/d \ln PwD'$ for vertically fractured wells with finite conductivity fractures. These graphs are similar to those shown for infinite conductivity vertically fractured wells with one exception. Here, we have also included the effect of varying dimensionless fracture conductivity $F_{CD} = (k_{fw}/kx_f)$. In the SPE nomenclature, F_{CD} is analogous to C_{fD} . Three values of F_{CD} , 0.05, 0.5, and 500 have been used. The value of 500 corresponds to a fracture of infinite conductivity whereas the value of 0.05 represents very low fracture conductivity. For each value of fracture conductivity, x_e/x_f values of 1, 2, 5, and 25 have been used.

Rate-Cumulative Production Decline-Type Curves. Another kind of graph which is commonly made by operations and field engineers is to plot rate $q(t)$, or normalized rate $q(t)/\Delta m(p)$ as a function of cumulative production. A recent paper on this topic is due to Callard.⁵ To investigate the character of these graphs, the

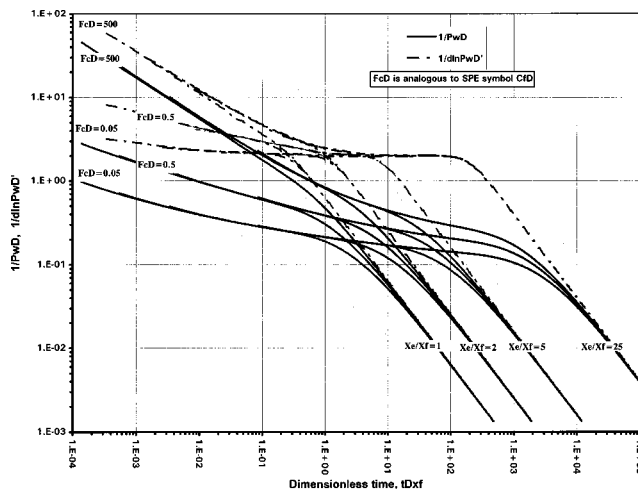


Fig. 14—Rate-time production decline-type curves for finite conductivity fracture using t_D based on x_f ($x_e/x_f = 1, 2, 5, 25$ and $F_{CD} = 0.05, 0.5, 500$).

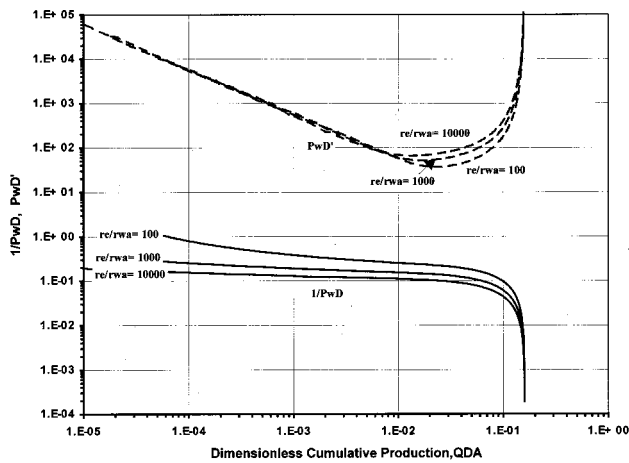


Fig. 15—Rate-cumulative production decline-type curves on log-log graph for radial systems using Q_D based on area ($r_e/r_{wa}=100, 1,000, 10,000$).

dimensionless groups $1/p_{wD}$ and the derivative of p_{wD} with respect to dimensionless cumulative production, Q_{DA} ($Q_{DA} = t_{DA}/p_{wD}$), were plotted as functions of Q_{DA} on log-log coordinates. Results in the form of type curves for radial flow systems for $r_e/r_{wa} = 100, 1,000,$ and $10,000$ are shown in **Figs. 15 and 16**.

Fig. 15 shows that during the transient flow period, separate $1/p_{wD}$ curves are obtained for each r_e/r_{wa} value. However, during pss flow they asymptotically merge into a single value of $Q_{DA} = 1/(2\pi)$ equal to 0.159, referred to as an anchor point value.

Fig. 16 is a Cartesian (linear) graph of the same $1/p_{wD}$ data as is used in Fig. 15. Notice that during the pss flow period, the $1/p_{wD}$ curves for each r_e/r_{wa} value become linear and converge at $Q_{DA} = 1/(2\pi)$. The significance of this attribute is that for an optimistic estimate of GIP the trajectory of the field data will undershoot the anchor point but will overshoot the anchor point for a pessimistic estimate of GIP. We find this graph very useful in obtaining estimates of GIP.

Fig. 17 shows $1/p_{wD}$ and the derivative of p_{wD} with respect to dimensionless cumulative production based on r_{wa}^2 , Q_{aD} ($Q_{aD} = t_{aD}/p_{wD}$) plotted against Q_{aD} . A notable feature of this graph is that $1/p_{wD}$, along with this derivative, forms an envelope. A vertical tangent to this envelope corresponds to the GIP. The derivative plot shows a negative unit slope line during the transient period but a positive slope during the pss period. These characteristics can be utilized to identify the transient and pss flow periods

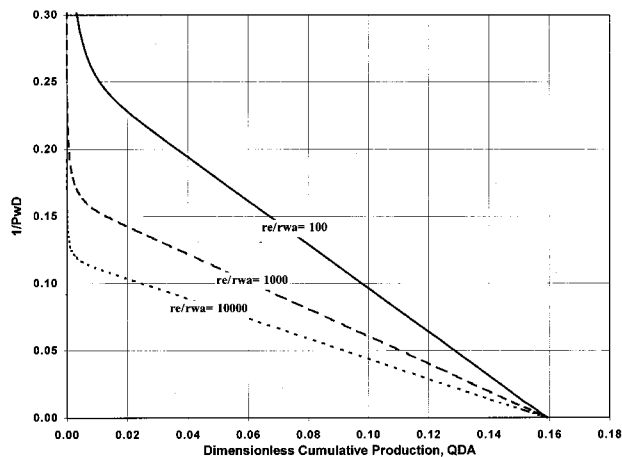


Fig. 16—Rate-cumulative production decline-type curves on Cartesian graph for radial systems using Q_D based on area ($r_e/r_{wa}=100, 1,000, 10,000$).

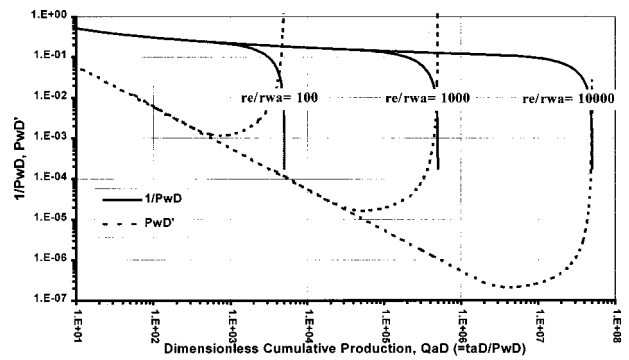


Fig. 17—Rate-cumulative production decline-type curves for radial systems using Q_D based on r_{wa} ($r_e/r_{wa}=100, 1,000, 10,000$).

and the transition between these flow periods. Moving to the left of this graph where the r_e/r_{wa} value decreases, $1/p_{wD}$ and its derivative curve become closer to one another forming a smaller size envelope. Although not shown, these two curves intersect one another for small values of r_e/r_{wa} . We utilize similar graphs for infinite and finite conductivity vertically fractured wells but they are not included in this paper. These characteristics of rate-cumulative type curves have proven to be advantageous for diagnostic and type-curve matching purposes.

Cumulative Production-Time Decline-Type Curves. We have also created cumulative production versus time decline-type curves for both the radial systems and for vertically fractured wells. We find such curves useful because field cumulative production data are often smoother than the corresponding rate data. Moreover, such curves have their own characteristics which can be used to our benefit in estimating reservoir parameters and reserves. Figs. 18 and 19 show these curves for wells with radial flow and for wells with finite conductivity fractures, respectively.

In Fig. 18, dimensionless cumulative production Q_{aD} is plotted as a function of dimensionless time based on wellbore radius using log-log coordinates. During the transient flow, a single curve is obtained for all r_e/r_{wa} values. It has a unit slope line except at dimensionless times less than about 100. During pss flow, the curves peel off and become flat for each value of r_e/r_{wa} .

Fig. 19 shows, for a fractured well, a log-log plot of dimensionless cumulative production Q_{aD} versus dimensionless time based on fracture half-length x_f . In this case, a separate curve is obtained for each value of dimensionless fracture conductivity. During transient flow, for each fracture conductivity value, a single curve is obtained for all x_e/x_f values. Their slopes range from 1 for low-conductivity fractures to 1/2 for infinite conductivity fractures. During pss flow, these curves peel off and become flat for each value of x_e/x_f .

Comments About These and Other Published Type Curves.

The type curves presented in **Figs. 9 through 19**, represent a new contribution to technology and add to recent work within the industry in advanced type-curve methods. For the sake of convenience and to differentiate them from other published decline-type curves, this new set of type curves will be referred to as *Agarwal-Gardner (AG) type curves*.

These AG type curves consider both the transient and the pss flow conditions, as well as the transition between the two, in a rigorous manner. They can be easily generated using analytical solutions and/or simulators for any desired flow system such as radial and vertically fractured wells. Analyses of tight gas wells require that a much longer transient period be considered, which is accommodated by these type curves. Alternately, published infinite and finite conductivity fracture type curves (such as those by Agarwal, Carter, and Pollock⁶ and Cinco *et al.*⁷) can also be used for the analysis of transient data. Infinite conductivity fracture

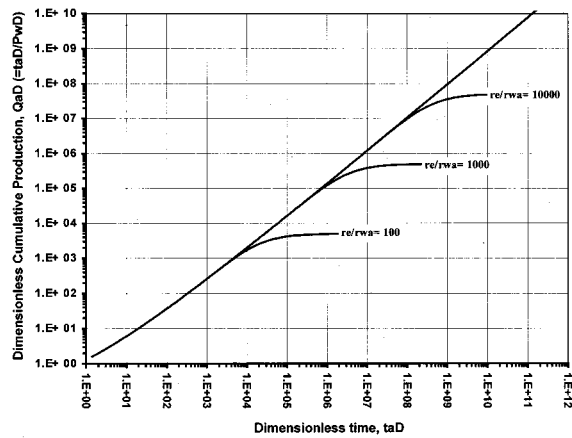


Fig. 18—Cumulative production-time decline-type curves for radial systems using t_D based on r_{wa} ($r_e/r_{wa} = 100, 1,000, 10,000$).

type curves published by *Gingarten et al.*⁸ can be used for transient as well as pss periods for vertically fractured wells. Similar comments apply to other published type curves.

Application of AG Type Curves. Type curves such as shown in Fig. 9 through 19 can be easily programed into a spreadsheet program. Modern spreadsheet programs provide a convenient way to history match field data to determine parameter values using these new type curves. A set of basic data is required to do the type-curve matching for gas wells regardless of which kind of type curve is used. The type of required data is listed below:

1. Reservoir data: Initial reservoir pressure (p_i), reservoir temperature (T), formation thickness (h), reservoir permeability (k), hydrocarbon porosity (ϕs_g).
2. Gas properties data: Tables of viscosity (μ), z factor, and gas compressibility (c_g) versus pressure including values of μ_i , z_i , and c_{gi} . Tables of real gas pseudopressure [$m(p)$] versus pressure.
3. Performance data: Well rate (q), bottomhole pressure (p_{BHP}), and cumulative gas production (Q) as a function of producing time (t).

Normally, the parameters to be determined are: GIP, formation flow capacity (kh), and wellbore skin or fracture length and conductivity for fractured wells.

Estimating GIP. With these new decline-type curves, we recommend that GIP be determined first. This is because the independent variable, Q_{DA} , used to estimate GIP, is independent of

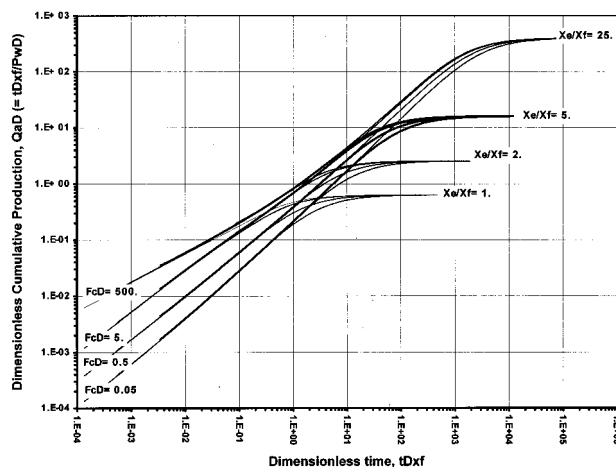


Fig. 19—Cumulative production-time decline-type curves for fractured wells using t_D based on x_f ($x_e/x_f = 1, 2, 5, 25$ and $F_{cD} = 0.05, 0.5, 500$).

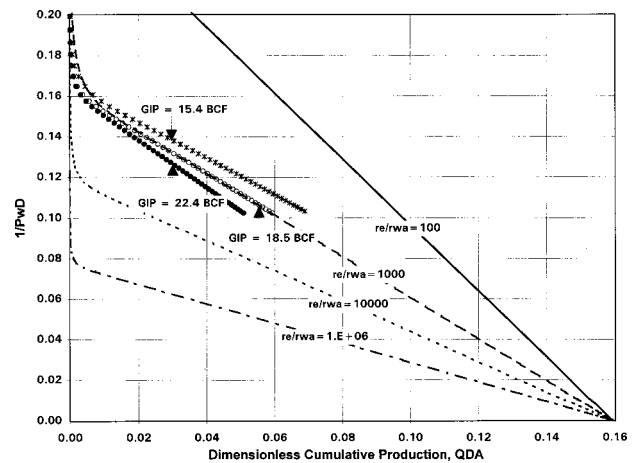


Fig. 20—Showing the effect of changing GIP estimates on rate-cumulative production decline-type curves on Cartesian graph for radial systems.

permeability, whereas the estimates of permeability, etc., are themselves dependent upon GIP.

It is only necessary to make an approximate initial estimate of GIP because convergence to a correct estimate of GIP is usually very rapid. The cumulative gas production can provide a lower-bound estimate for GIP, whereas a volumetric estimate obtained from petrophysical data could provide an upper-bound estimate. A value somewhere between the two would suffice for an initial estimate.

Fig. 20 shows the rate-cumulative production decline-type curves. It illustrates the concept of graphically estimating GIP based on responses to changes in GIP values relative to the type curves. In Fig. 20, we use values of plus and minus 20% of the true value of GIP to showcase this sensitivity. Notice that with the correct GIP, the data follow the trajectory of one of the $1/P_{wD}$ rays. It does not matter which of these rays are used, all focus to the same anchor point value of $1/(2\pi)$ on the Q_{DA} axis.

Estimating Formation Flow Capacity, kh . Fig. 21 shows rate-time production decline-type curves and illustrates the concept of graphically estimating kh based on responses to changes in kh values relative to the type-curve values. In Fig. 21, we use kh values of 2.0 and 0.5 md ft, which are twice and 1/2 the true value of 1.0 md ft, to demonstrate the sensitivity to changes in formation flow capacity, kh .

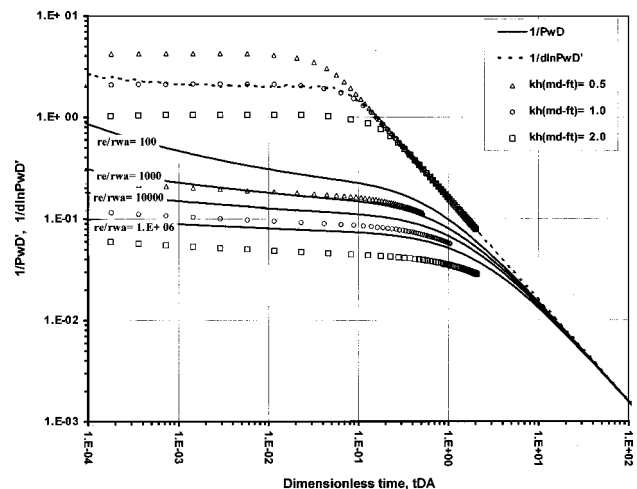


Fig. 21—Showing the effect of changing kh estimates on Rate-Time Log-Log production decline-type curves for radial systems using t_D based on area.

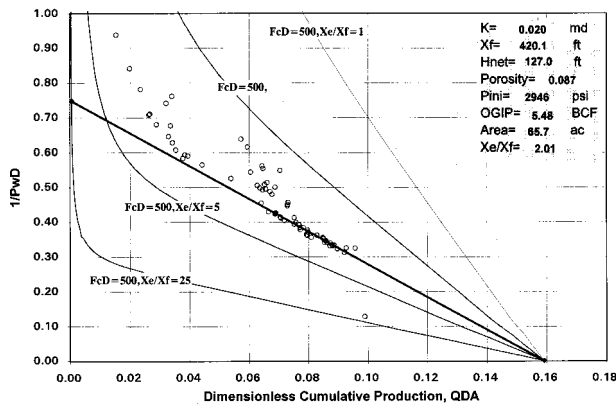


Fig. 22—Application of field data to estimate GIP using rate-cumulative production decline-type curves on Cartesian graph for finite conductivity fracture using Q_D based on area.

Field Application of AG Type Curves. Figs. 22 and 23 show history matched parameter estimates for GIP, permeability, etc., for an infill gas well in the low-permeability Red Oak sand of southeastern Oklahoma. The well was drilled in December, 1991, has slightly over six years of production history with a cumulative production of 1.9 Bscf. These production data are typical of that obtained from industry or field databases and the noise or inaccuracies in measured or reported data is reflected in the plotted dimensionless data.

Fig. 22 shows that the plot of $1/p_{wD}$ vs. Q_{DA} converges nicely to the GIP anchor point and that the estimate of GIP can be used with some confidence. The character of the derivative data on the plot of $1/p_{wD}$ vs. t_{DA} (Fig. 23) clearly shows that the well has transitioned to boundary-dominated flow. This plot also illustrates a match for estimating permeability, fracture half-length, and dimensionless fracture conductivity. Only minor modifications to the parameter values obtained from this type-curve match were needed to match the well's history using a finite-difference simulator.

Fig. 24 is a plot of the same production data on a Palacio-Blasingame type curve. The estimates of GIP between the two type curves are in excellent agreement, differing by less than 3%. There is, however, ambiguity about which transient stem to match the data with for calculating permeability and wellbore skin. This illustrates a benefit of using these new type curves for low-permeability fractured wells which typically have long linear or bilinear transient flow periods.

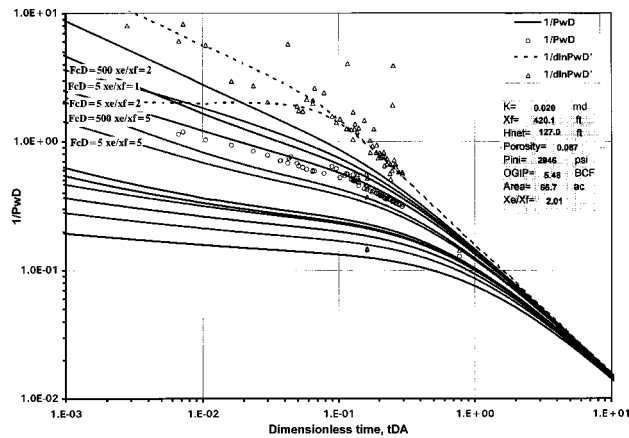


Fig. 23—Application of field data to estimate kh using rate-time production decline-type curves for finite conductivity fractures using t_D based on area.

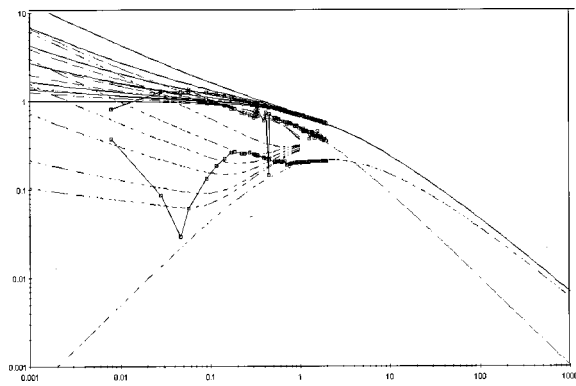


Fig. 24—Application of field data to estimate GIP and kh using Palacio-Blasingame radial system type curves.

Summary and Conclusions

1. A new set of rate-time, rate-cumulative, and cumulative-time production decline-type curves and their associated derivatives have been developed using pressure transient analysis concepts and are presented in this paper.

2. They have been developed for radial systems and vertically fractured wells with infinite and finite conductivity fractures. These production decline curves are, to our knowledge, the first to be published in this format especially for fractured wells.

3. These new production decline-type curves represent an advancement over previous work in that a clearer distinction can be made between transient and boundary-dominated flow periods.

4. They provide a practical tool to field engineers for estimating gas (or oil) -in-place as well as to estimate reservoir permeability, skin effect, fracture length, and fracture conductivity. Also, because this technology can be easily programed into an electronic spreadsheet, it can more readily be used.

5. These type curves enable us to utilize routinely collected production data and those commonly available from industry databases in the absence of costly pressure transient data.

6. These concepts can be extended to other well and/or reservoir models such as horizontal wells or naturally fractured reservoirs, to name a few.

Nomenclature

- A = drainage area, sq ft
- b = Arp's decline curve exponent
- c_g = gas compressibility, 1/psi
- $(c_g)_i$ = gas compressibility at initial reservoir pressure, 1/psi
- c_t = total system compressibility, 1/psi
- D_{it} = Arp's dimensionless decline rate
- e = 2.71828, Napierian constant
- $F_{CD} = C_{fD}$ = dimensionless fracture conductivity
- G_i = initial gas-in-place, MMSCF or BSCF
- G_p = cumulative gas produced, MMSCF or BSCF
- k = effective permeability to gas, md
- k_f = fracture permeability, md
- $m(p)$ = real gas pseudo pressure, psia^2/cp
- $\Delta[m(\bar{p})]$ = $m(p_i) - m(\bar{p})$, psia^2/cp
- $\Delta[m(p)]$ = $m(p_i) - m(p_{BHP})$, psia^2/cp
- p_{BHP} = bottomhole producing pressure, psia
- \bar{p} = average reservoir pressure, psia
- p_i = initial reservoir pressure
- p_{wD} = dimensionless wellbore pressure
- q_i = initial flow rate, MSCF/D
- $q(t)$ = flow rate, MSCF/D
- $Q(t)$ = cumulative production, MMSCF
- Q_{DA} = dimensionless cumulative production based on area (A)
- Q_{aD} = dimensionless cumulative production based on r_{wa}^2 , or x_f^2

r_{wa} = effective wellbore radius, ft
 r_e = reservoir radius, ft
 s = skin factor
 t = time, days
 T = reservoir temperature, degrees Rankine
 t_a = pseudoequivalent time
 t_e = equivalent time [cumulative(t)/ $q(t)$], days
 t_{DA} = dimensionless time based on area, A
 t_{aD} = dimensionless time, based on r_{wa}^2
 t_{DXf} = dimensionless time, based on x_f^2
 w = fracture width, ft
 x_e = distance from well to reservoir boundary (Cartesian coordinate system)
 x_f = fracture half length, ft
 z_i = initial gas compressibility factor
 \bar{z} = gas compressibility factor at average pressure

Greek Letters

ϕ = hydrocarbon porosity, fraction
 λ = Carter's drawdown variable
 μ = viscosity, cp
 π = 3.14159

Acknowledgments

The authors wish to thank the Amoco Production Company for permission to publish this paper. We also express appreciation for the company's support for the creation, the dissemination, and the application of this technology.

References

- Arps, J.J.: "Analysis of Decline Curves," *Trans.*, AIME (1945) **160**, 228.
- Fetkovich, M.J.: "Decline Curve Using Type Curves," *JPT* (June 1980) 1065.
- Carter, R.D.: "Type Curves for Finite Radial and Linear Gas Flow Systems: Constant Terminal Pressure Case," *SPEJ* (October 1985) 719.
- Fraim, M.L., and Wattenbarger, R.A.: "Gas Reservoir Decline-Curve Analysis Using Type Curves with Real Gas Pseudopressure and Normalized Time," *SPEFE* (December 1987) 620.
- Callard, J.G.: "Reservoir Performance History Matching Using Rate/Cumulative Type-Curves," paper SPE 30793 presented at the 1995 SPE Annual Technical Conference and Exhibition, Dallas, 22–25 October.
- Agarwal, R.G., Carter, R.D., and Pollock, C.B.: "Evaluation and Performance Prediction of Low-Permeability Gas Wells Stimulated by Massive Hydraulic Fracturing," *JPT* (March 1979) 362; *Trans.*, AIME **267**.
- Cinco, L.H., Samaniego, V.F., and Dominguez, A.N.: "Transient Pressure Behavior for a Well with a Finite-Conductivity Vertical Fracture," *SPEJ* (August 1978) 253.
- Gringarten, A.C., Ramey, Jr., H.J., and Raghavan, R.: "Unsteady-State Pressure Distributions Created by a Well With a Single Infinite-Conductivity Vertical Fracture," *SPEJ* (August 1974) 347; *Trans.*, AIME **257**.

Appendix

$$t_e = Q(t)/q(t), \quad (A-1)$$

$$t_a = \frac{1}{q(t)} (\mu c_g)_i \int_0^t \frac{q(t') dt'}{\mu(\bar{p}) c_g(\bar{p})} = \frac{1}{q(t)} (\mu c_g)_i \frac{Z_i G_i}{2 p_i} \Delta[m(\bar{p})], \quad (A-2)$$

where $\Delta[m(\bar{p})] = m(p_i) - m(\bar{p})$,

$$\text{and } m(p) = 2 \int_0^p \frac{p' dp'}{\mu(p') z(p')}, \quad (A-3)$$

$$t_{aD} = \alpha t, \quad (A-4)$$

$$t_{aD} = \alpha t_a, \quad (A-5)$$

where $\alpha = (2.637 \times 10^{-4})(24)k/\phi(\mu c_t)_i r_{wa}^2$,

$$\frac{1}{p_{wD}} = \frac{1422 T q(t)}{k h \Delta m(p)}, \quad (A-6)$$

$$p_{wD} = (p_D + s), \quad (A-7)$$

$$Q_{aD} = \frac{t_{aD}}{p_{wD}} = \frac{9.0 T}{\phi h \Delta m(p) r_{wa}^2} \int_0^t \frac{q(t') dt'}{\mu(\bar{p}) c_g(\bar{p})}, \quad (A-8)$$

and

$$Q_{aD} = \frac{4 \cdot 50 T z_i G_i \Delta m(\bar{p})}{\phi h r_{wa}^2 p_i \Delta m(p)}, \quad (A-9)$$

where $\Delta m(p) = [m(p_i) - m(p_{BHP})]$.

Dimensionless times in Eqs. A-3 through A-5 are based on r_{wa}^2 . These are multiplied by r_{wa}^2/A to convert them so that they are based on the area A . For example, $t_{DA} = t_{aD}(r_{wa}^2/A)$, and $Q_{DA} = Q_{aD}(r_{wa}^2/A) = t_{DA}/p_{wD}$.

SI Metric Conversion Factors

acre	× 4.046	873 E+03	= m ²
bbl	× 1.589	873 E-01	= m ³
cp	× 1.0*	E-03	= Pa·s
ft	× 3.048*	E-01	= m
md ft	× 3.008	142 E+02	= μm ²
psi	× 3.048*	E+00	= kPa
psi ⁻¹	× 1.450	377 E-04	= Pa ⁻¹
cu ft	× 2.831	685 E-02	= m ³
md	× 9.869	233 E-04	= μm ²
R	× 5/9		= K

*Conversion factors are exact.

SPERE

Ram G. Agarwal is a staff petroleum engineering associate for BP Amoco in Houston, where he specializes in pressure transient testing and gas reservoir engineering. e-mail: agarwarg@bp.com. Agarwal holds a BS degree in petroleum from the Indian School of Mines, a Diploma from Imperial College in petroleum reservoir engineering, and a PhD degree in petroleum engineering from Texas A&M U. in College Station, Texas. He has served on several SPE committees, including the Distinguished Author Series Committee. Agarwal was elected a Distinguished Member of SPE in 1998 and was named recipient of the Formation Evaluation Award in 1999. **David C. Gardner** is a staff petroleum engineer for BP Amoco in Houston working in the areas of hydraulic fracturing and gas reservoir engineering. e-mail: gardnedc@bp.com. He holds a BS degree in chemistry and an MS degree in chemical engineering, both from Brigham Young U. in Provo, Utah. **Stanley W. Kleinstiber** is a senior petroleum engineer for Malkewicz Hueni Assocs. in Golden, Colorado, where he specializes in reservoir evaluation studies. e-mail: skleinst@mhausa.com. Previously, he worked for Amoco Production Co. as a reservoir engineering consultant and technology coordinator. He holds a BS degree in petroleum engineering from the U. of Oklahoma in Norman, Oklahoma. **Del D. Fussell** was a manager of engineering technology in Amoco's Denver office before retiring from the company in 1997. e-mail: ddfussell@worldnet.att.net. Previously, he worked at Amoco's offices in Tulsa, Oklahoma, Houston, and Cairo. He holds BS and MS degrees in chemical engineering from the U. of Nebraska in Lincoln and a PhD degree from Rice U. in Houston. He served as Chairman of the SPE Forum on Gas Technology in 1995.